Evidence of ratchet effect in nanowires of a conducting polymer

A. Rahman, M. K. Sanyal, R. Gangopadhayy, A. De, and I. Das
Saha Institute of Nuclear Physics, 1/AF Bidhannagar, Kolkata 700 064, India.
(Dated: February 2, 2008)

Ratchet effect, observed in many systems starting from living organism to artificially designed device, is a manifestation of motion in asymmetric potential. Here we report results of a conductivity study of Polypyrrole nanowires, which have been prepared by a simple method to generate a variation of doping concentration along the length. This variation gives rise to an asymmetric potential profile that hinders the symmetry of the hopping process of charges and hence the value of measured resistance of these nanowires become sensitive to the direction of current flow. The asymmetry in resistance was found to increase with decreasing nanowire diameter and increasing temperature. The observed phenomena could be explained with the assumption that the spatial extension of localized state involved in hopping process reduces as the doping concentration reduces along the length of the nanowires.

PACS numbers: 72.80.Le, 72.20.Ee, 73.23.Hk, 73.63.Nm

Flow of particles becomes direction sensitive in presence of a ratchet potential whose principal feature is loss of inversion symmetry [1, 2, 3, 4, 5, 6, 7, 8, 9, 10, 11]. Depending upon the origin of asymmetric potential and fluctuating force several kinds of ratchets are observed ranging from molecular motors [3] in which proteins move in a deterministic way along filaments, to electron pumps [5] engineered in semiconductor channels. Ratchet effect has been utilized in diverse fields like in the process of particle separation [8] and in optical tweezing [9]. We report here an evidence of ratchet potential formation in nanowires of a conducting polymer. The resistance of these nanowires can differ by several kilo-Ohms as the direction of current flow along the length is reversed. This effect become more pronounced with decrease of diameter of the nanowires and increase in temperature.

Strong dependence of conductivity (σ) of conjugated polymers on doping concentration (c), defined as number of carriers per monomer, is indeed an important phenomenon to be exploited in polymer electronics. Experimentally observed seven orders of magnitude increase in σ due to increase of c from 0.005 to 0.2 has been explained with a variable range hopping (VRH) theory by invoking doping concentration dependent size of the extent of localized region that vary from 1 to 5 nm [12]. We have used a simple preparation process in which the gradient of c along polymer wires could be controlled by performing the polymerization reaction in a confined environment, provided by pores of membranes. Polycarbonate membranes (Whatman Inc.) of thickness $\sim 6\mu m$ was placed between two compartments of a chemical cell having aqueous solution of pyrrole monomer (0.1M) in one side and ferric chloride ($FeCl_3$) (0.5M) as oxidizing agent in the other compartment. The oxidizing agent $FeCl_3$ acts as polymerization agent in formation of Polypyrrole and provides dopant (counter anion) Cl^-. The atomic ratio of Cl to N determines the degree of dopant and one obtains $c = 0.33$ for fully doped Polypyrrole [13].

Several membranes each having uniform pore diameter ranging from 30 nm to 200 nm were used for growing nanowires of different diameters. Each membrane was first exposed to monomer to fill the pores and then after about five minutes $FeCl_3$ solution was allowed to flow in the pores. Polymerization raction takes place within each pore as $FeCl_3$ start diffusing through these pores towards the compartment containing the monomer. This diffusion process of the oxidizing agent create a profile of c that reduces continuously along the length of the nanowire as shown in schematic diagram Fig. 1(a). The results of Scanning Electron Microscopy (SEM) and Transmission Electron Microscopy (TEM) measurements performed at various stages of this growth process indicated that polypyrrole preferentially nucleate to the pore wall forming tubes first and then the tubes get converted into solid wire (Fig. 1(b)) as observed earlier [14].We have extracted dopant (Cl^-) concentration as a function of depth using Secondary Ion Mass Spectroscopy (SIMS) technique. SIMS profiles were extracted for Cl and N from both faces of membranes to confirm consistency of the profiles. More than two orders of magnitude variation of c was observed along the length of nanowires having 30 nm diameter and constant doping was obtained only at a depth of 400 nm from $FeCl_3$ compartment. But for 200 nm diameter nanowires the variation was found to be only one order of magnitude and constant doping was obtained within 100 nm depth (Fig.1(c)).

To determine the current-voltage (I-V) characteristics of nanowires a direct current was swept between positive and negative maximum values across the membrane by applying silver paste on both sides. The nanowires in the membrane get connected in parallel and the voltage developed across the nanowires was measured in this pseudo four-probe geometry (Fig. 2(a) (inset)). In Fig. 2(a) we have shown typical resistance data of a membrane having 30nm nanowires where direction of current (100μ Amp for 297.5K, 240K and 1μ Amp for 133K and 64K)

is reversed at $t = 50$ sec. Significant difference ($\sim$ 67 kilo-ohms) in measured value of resistance was observed even at 64K data though the effect was found to be more at higher temperatures. In Fig. 2(b) we have presented I-V data measured with positive (I^+), and negative (I^-), current to illustrate the effect of temperature. We have repeated the measurement with conducting copper tape and gold sputtered contact and obtained similar results. This observation and the fact that observed resistance asymmetry reduces with lowering of temperature rules out the possibility that asymmetry in resistance is arising due to the formation of Schöttky barrier in the contact. We observed that best quality samples could be prepared by cooling the membrane at liquid nitrogen temperature right after the nanowire fabrication, as suggested [16]. Net current $I_{net} = (|I^+| - |I^-|)$ of one such 30nm sample measured with gold sputtered contact at 28K temperature is shown in inset of Fig. 2(b). This quenching procedure reduces the mobility of dopants and contribution of ionic conductivity in total current become much less even above 200K temperature.

Below 200K electronic nature of transport dominates and one expects to observe $ln\rho \propto (T_0/T)^\beta$ dependence of resistivity. The exponent β takes the value of 1/4 for Mott 3D VRH [17] but approaches the value of 1/2 if Coulomb interactions create a gap as argued by Efros and Shklovskii [18]. Based on a heuristic calculation a cross over function has been proposed as [19]

$$f(x) = \frac{1 + [(1+x)^{1/2} - 1]/x}{[(1+x)^{1/2} - 1]^{1/2}} \qquad (1)$$

with $x = T/T_x$. This function exibit smooth crossover from Mott $f(x) \propto x^{-1/4}$ for $x \gg 1$ to Efros-Shklovskii $f(x) \propto x^{-1/2}$ for $x \ll 1$ behaviors. In Fig. 3(a) we have shown variation of resistance of a quenched 30nm sample with gold sputter contact as a function of temperature and a fit to Eq. (1) that gives the value of T_x as 9K. The deviation of data at higher temperature from $f(x)$ is expected [19] due to direct thermal activation. This fit clearly indicates that for the measured temperature range (25K to 300K) we are in Mott's 3D variable range regime as confirmed in the fit shown in the inset of Fig. 3(a). It has been shown [20] that Mott's $T^{-1/4}$ VRH conduction law persists even in intrastate interacting electron system. It may be noted that T_0 obtained in both fittings is consistent [19]. We also observed $\beta = 1/4$ in all the non-quenched samples with silver past contact and some of the data and corresponding fits are shown in Fig. 3(b). For 30nm unquenched sample voltage goes into nonlinear region as the resistance grows substantially at lower temperature ($< 175K$). Taking value of localization length $(\alpha^{-1}) \sim 0.2nm$ [12, 21] the parameters density of states ($N(E_F)$), hopping range (R_{hop}) and hop activation energy (W) comes out to be as $6.2\times10^{22}, 7.68\times10^{21}, 2.55\times10^{21}, 1.24\times10^{20}\ cm^{-3}eV^{-1}$; $0.45, 0.77, 1.02, 2.17\,nm$ and $40, 68, 88, 188\,meV$ for bulk, 200nm, 50nm and 30nm sample respectively.

The observed electrical transport properties of polypyrrole nanowires and ratchet effect reported here can be explained by considering a simple model having unconnected linear array of nanospheres, representing the extent of the localized states, with decreasing diameter (d) as c reduces along the length of the nanowires from $x = 0$ to $x = L$ (refer Fig. 4(a)). This variation gives rise to gradual increase in the bare energy level spacing and charging energy ($Q^2/4\pi\epsilon_0\epsilon d$) ($\epsilon$ is the static dielectric constant) with reducing value of diameter (d) of the nanospheres that hinder the symmetry of the VRH charge transport mechanism [15, 22, 23, 24, 25]. In Fig. 4(b) we have quantified the inherent asymmetric hopping process in our nanowires by considering forward and reverse bias hopping of charge between two adjacent nanospheres of two different sizes signifying different extent of localized sites. As a bias is applied to the system, the charges start to hop from one site to another. In a nanosphere the energy of an added electron depends on both charging energy, and the bare energy level spacing [26]. The size asymmetry of adjacent nanosphere introduces observed ratchet effect [27, 28, 29] in the flow of charges here. Let the energy of an added electron for the larger left and smaller right nanospheres are U_{cL} and U_{cR} respectively ($U_{cL} < U_{cR}$). The effective barrier height on the right side for hopping towards left is Δ_R and that for the left side is Δ_L where $\Delta_R = \Delta_L - U_d$. The difference charging energy $U_d = (U_{cR} - U_{cL}) \equiv Q^2/(4\pi\epsilon)\left(\frac{1}{d_R} - \frac{1}{d_L}\right)$ where d_R and d_L are diameter of right and left sphere respectively. Under the application of positive (negative) bias the hopping rates (transition probabilities) $\Gamma_R^\pm$ and $\Gamma_L^\pm$ can be expressed as

$$\Gamma_R^\pm = \Gamma_0\ exp\{-(\Delta_R \mp 0.5V + |\Delta_R \mp 0.5V|)/(2kT)\} \quad (2)$$

from right to left and

$$\Gamma_L^\pm = \Gamma_0\ exp\{-(\Delta_L \pm 0.5V + |\Delta_L \pm 0.5V|)/(2kT)\} \quad (3)$$

from left to right, where V is the total potential drop across the two sites [25, 30]. Current for positive (negative) bias can be written as $I^\pm = Qb\left(\Gamma_R^\pm - \Gamma_L^\pm\right)$ where Q is the amount of charge that hops and b is the distance between the two hoping sites. A very small value of U_d can introduce significant asymmetry in the current.

A parameter ϕ defined as $\phi = (|I^+| - |I^-|)/(|I^+| + |I^-|)$ has been used to quantify the observed asymmetry where $|I^+|$ and $|I^-|$ represent magnitude of forward and reverse current for same magnitude of voltage, respectively. The measured values of ϕ was found to decrease appreciably with increasing diameter of nanowires - for example, at room temperature ϕ come out to be around 0.3, 0.12, 0.012 and 0.008 for samples having nanowires of nominal diameter of 30, 50, 100 and 200 nm respectively. The

values of ϕ become zero for bulk sample measured using same geometry and electrical contacts. The values of ϕ was found to increase with increasing temperature for all nanowires, as shown in the lower inset of Fig. 4(c) for the samples having nanowires of 30 nm diameter. In our model even for $U_d = 0.4$ meV we get $\phi = 0.2$ at 300K (taking barrier height= $188meV$, voltage drop across a barrier = $2meV$). The observed increase in ϕ with increasing temperature (Fig. 4(c) lower inset) is generally not expected in the hopping process. In the first approximation ϕ should have been independent of temperature as in polypyrrole dielectric constant ϵ is known to be proportional to T^{-1} [31] and that would have made U_d proportional to T. In Fig. 4(c) we have shown variation of ϵ of a 30nm sample with temperature obtained from the peak in the capacitance value measured as a function of frequency [31] (refer upper inset in Fig. 4(c)). We get $\epsilon \propto T^{-1.4\pm0.06}$ and this in turn provide a qualitative explanation of increase in ϕ with temperature. For example in the above calculation U_d now becomes 0.057meV at 74K and that gives a value of ϕ as 0.02. This is close to the experimental value of 0.01 shown in lower inset of Fig. 4(c). It should be mentioned here that ϵ of water solvent was found to be proportional to $T^{-1.5}$ instead of T^{-1} as dipole rotation get hindered [32] and similar hinderance may be existing for our polypyrrole nanowires formed in confined geometry.

In conclusion, the observed ratchet effect in electrical transport of polypyrrole nanowire could be explained with a simple model having growing extent of localization sites along the nanowire. One should be able to make charging rectifier in polymer nanowires simply by reducing the radius of the nanospheres further from the present value of 30 nm used here.

Authors would like to thank Prof. A. K. Sood for valuable discussions. Authors are grateful to Prof. P. Chakraborty and Prof. A. Ghosh for their help in SIMS and capacitance measurements, respectively.

[1] P. Reimann, M. Goifoni, and P. Hanggi, Phys. Rev. Lett. **79**, 10 (1997).
[2] P. Reimann, Phys. Rep. **361**, 57 (2002).
[3] Frank Julicher, Armand Ajdari, and Jacques Prost, Rev. Mod. Phys. **69**, 1269 (1997).
[4] H. Linke, T. E. Humphrey, A. Lfgren, A. O. Suskov, R. Newbury, R. P. Taylor, P. Omling, Science, **286**, 2314 (1999).
[5] M. Switkes, C. M. Marcus, K. Campman, A. C. Gossard, Science, **283**, 1905 (1999).
[6] R. D. Astumian, Science, **276**, 917 (1997).
[7] K. Kitamura, M. Tokunaga, A. H. Iwane, T. Yanagida, Nature, **397**, 129 (1999).
[8] Sven Matthias, and Frank Mller, Nature, **424**, 53 (2003).
[9] L. P. Faucheux, L. S. Bourdieu, P. D. Kaplan and A. J. Libchaber, Phys. Rev. Lett. **74**, 1504 (1995).
[10] M. Stopa, Phys. Rev. Lett. **88**, 146802 (2002).
[11] J. Lehmann, S. Kohler, P. Hnggi, and A. Nitzan, Phys. Rev.Lett. **88**, 228305 (2002).
[12] H. C. F. Martens, I. N. Hulea, I. Romijn, H. B. Brom, W. F. Pasveer, and M. A. Michels, Phys. Rev. B. **67**, 121203(R) (2003).
[13] Steven P. Armes, Synthetic Metals, 365, 20 (1987); Chun-Guey Wu and Ching- Yuh Chen, J. Mater. Chem, 1409, 7 (1997),
[14] C. R. Martin, Science, 266, 1961 (1994), Adv. Mater. 3, 457 (1991), Chem. Mater. **6**, 1627 (1994).
[15] J. A. Reedijk, H. C. F. Martens, H. B. Brom, and M. A. J. Michels, Phys. Rev. Lett. **83**, 3904 (1999).
[16] M. Ahlskog, M. Reghu, A. J. Heeger, T. Noguchi and T. Ohnishi, Phys. Rev. B. **55**, 15529 (1996).
[17] N. F. Mott and E. A. Davis, *Electrnic Process in Non-crystalline Materials* (Oxford University Press, Oxford, 1979)
[18] B. I. Shklovskii and A. L. Efros, *Electronic Properties of Doped Semiconductor* (Springer-Verlag, Berlin, 1984)
[19] A. Aharony, Y. Zhang, and M. P. Sarachik, Phys. Rev. Lett. **68**,3900 (1992).
[20] Hiroshi Kamimura and Hideo Aoki, *The Physics of Interacting Electrons in Disordered Systems* (Clarendon Press, Oxford, 1989)
[21] Ramadhar Singh, R. P. Tandon and Subhas Chandra, J. Phys: Condens. Matter **5**, 1313 (1993).
[22] A. B. Kaiser, Rep. Prog. Phys. **64**, 1 (2001).
[23] H. C. F. Martens, O. Hilt, H. B. Brom, P. W. M. Blom and J. N. Huiberts, Phys. Rev. Lett. **87**,086601 (2001).
[24] W. A. Schooneveld, J. Wildeman, D. Fichou, P. A. Bobbert, B. J. van Wees and T. M. Klapwijk, Nature **404**, 977 (2000).
[25] H. Cordes, S. D. Baranovskii, K. Kohary, P. Thomas, S. Yamasaki, F. Hensel and J. -H. Wendorff, Phys. Rev. B, **63**, 094201 (2001).
[26] Yigal Meir, Need S. Wingreen, and Patrick A. Lee, Phys. Rev Lett. **66**, 3048 (1991).
[27] K. W. Kehr, K. Mussawisade, T. Wichmann, and W. Dieterich, Phys. Rev. E. **56**, R2351 (1997).
[28] Markus Porto, Phys. Rev. E, **64**, 021109 (2001).
[29] J. Fransson, Phys. Rev. B, **69**, 201304(R) (2004).
[30] A. Millar, and E. Abrahams, Phys. Rev. **120**, 745 (1960).
[31] Ramadhar Singh, Amarjeet K. Narula and R. P. Tandon, J. App. Phys. **80**, 985 (1996).
[32] P. M. Chaikin, P. Pincus, and S. Alexander, J. Colloid and Interface Sci. **89**, 555 (1982).

Figure captions:

FIG. 1: (a) Schematic diagram of the set-up used to prepare nanowires of conducting polymer in nanopores of membranes. (b) SEM image of a bundle of nanowire formed in this process. (c) Cl and N profiles obtained from SIMS measurements for 30nm and 200nm nanowires are shown in the upper panel as a function of length. Ratio between these two profiles normalized to maximum doping of 0.33 is shown in the lower panel.

FIG. 2: (a) Difference in resistance value for forward and reverse bias current of 30 nm nanowires shown before and after switching the polarity of the bias at t=50sec. Electrical connections for measuring current-voltage characteristics have been shown in the inset. (b) Voltage developed across the nanowires as a function of forward (dashed line) and reverse (continuous line) bias current taken at various temperatures. Low temperature data has been multiplied by constant factors, as shown, to use the same scale. Higher temperature data have been shifted vertically for clarity. Net current is plotted as a function of voltage for liquid nitrogen quenched 30nm sample having gold contact (inset).

FIG. 3: (a)Resistance vs temperature plot and fit to Eq. (1) to determine crossover from $T^{-1/4}$ regime to $T^{-1/2}$ regime. Same data plotted in inset to show that $T^{-1/4}$ law is valid in our measurement range. (b) Same plot as inset of (a) for samples having different diameters.

FIG. 4: (a) Schematic representation of expected increase of the extent of localized states along the length (L) of nanowires represented by unconnected conducting nanospheres of increasing diameters is shown. Difference in charging energy due to an added electron on these nanospheres has been indicated. (b) Hopping model used to explain the resistance asymmetry is shown. (c) Dielectric constant obtained from frequency dependent capacitance data (shown in upper inset) as a function of temperature is plotted in Log-Log scale. The parameter ϕ that quantifies the ratchet effect is plotted as a function of temperature (in lower inset).

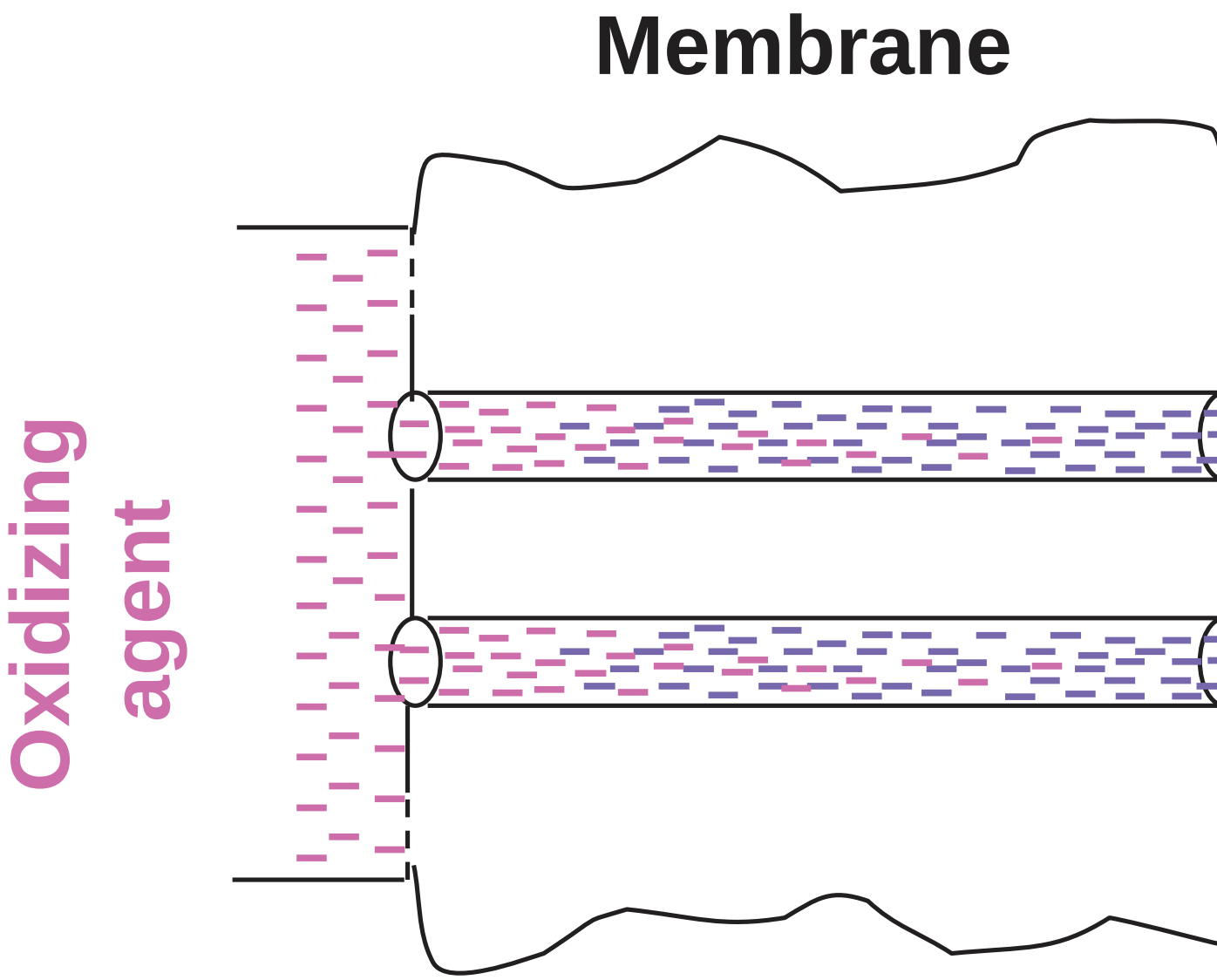
Membrane
Oxidizing agent

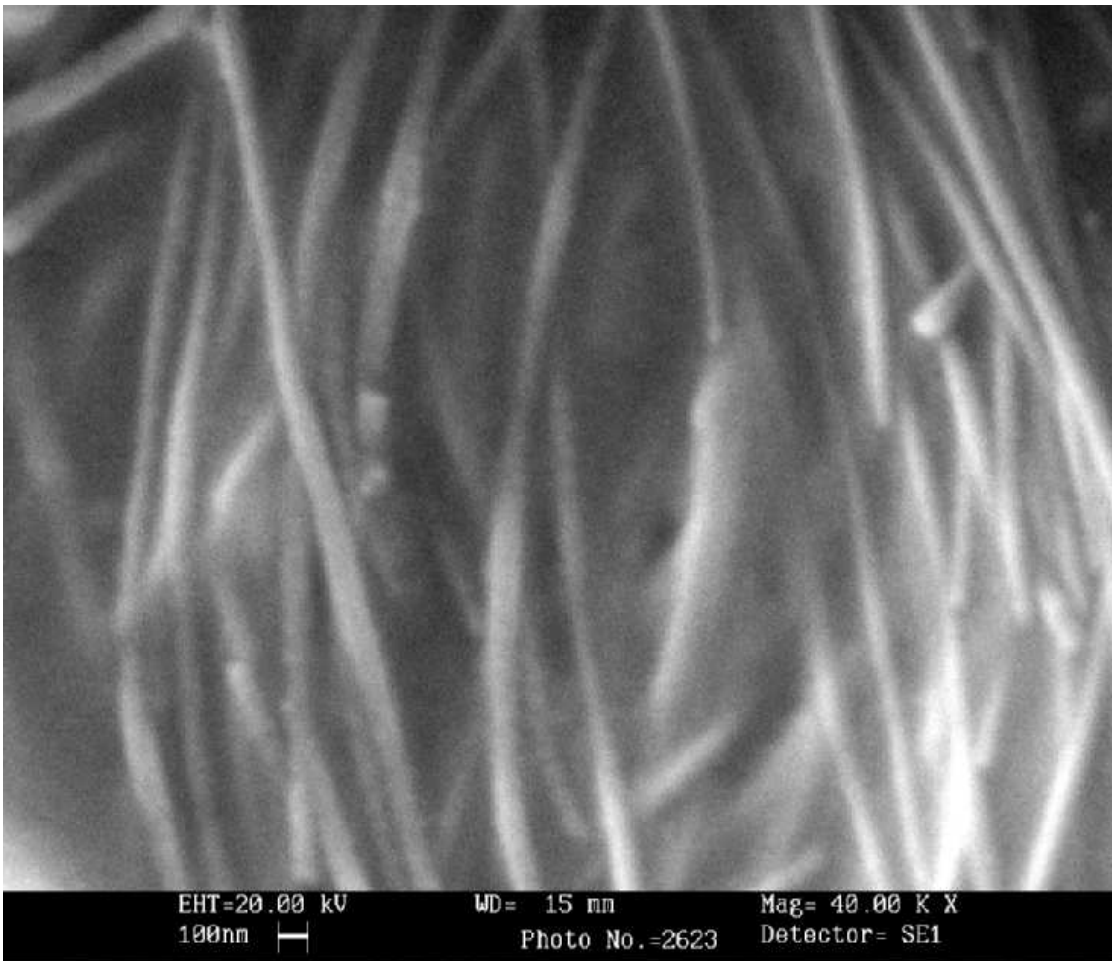
EHT=20.00 kV
WD= 15 mm
Mag= 40.00 K X
100nm
Photo No.=2623
Detector= SE1

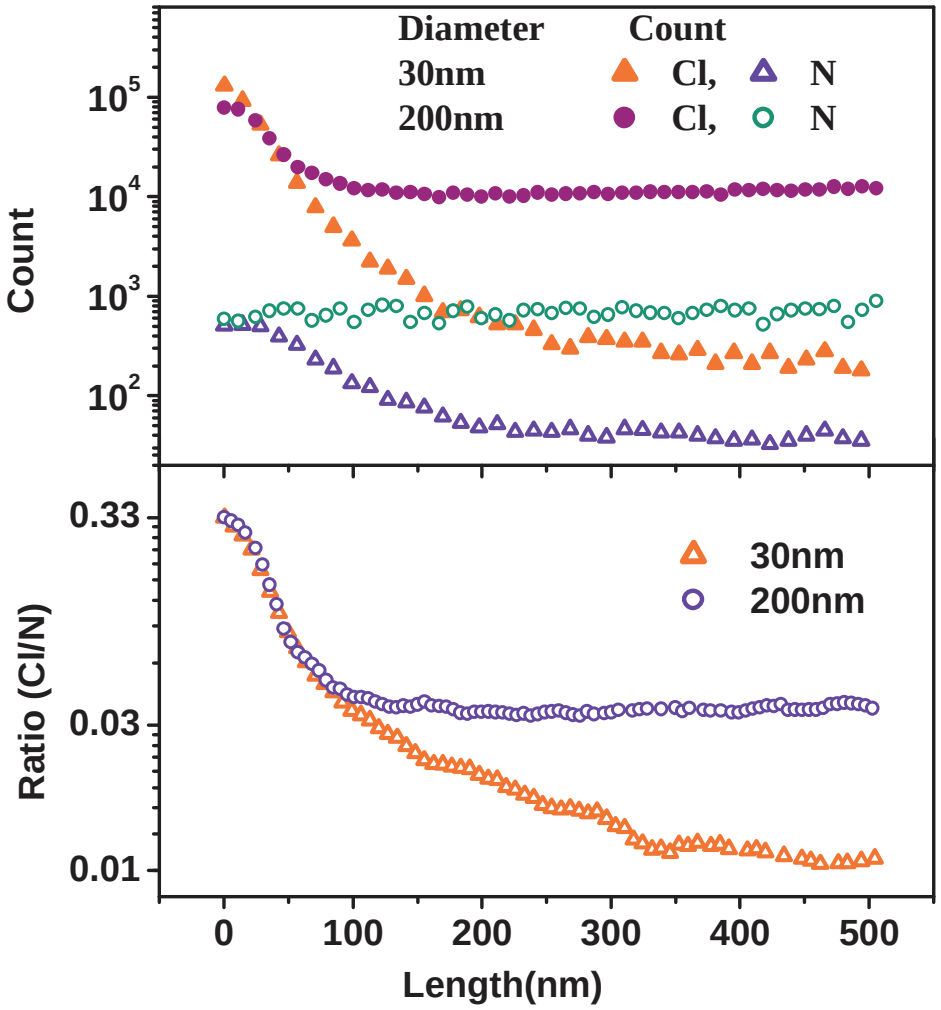
Diameter
Count
30nm
Cl,
N
200nm
Cl,
N
Count
10^5
10^4
10^3
10^2
0.33
0.03
0.01
Ratio (Cl/N)
30nm
200nm
0
100
200
300
400
500
Length(nm)

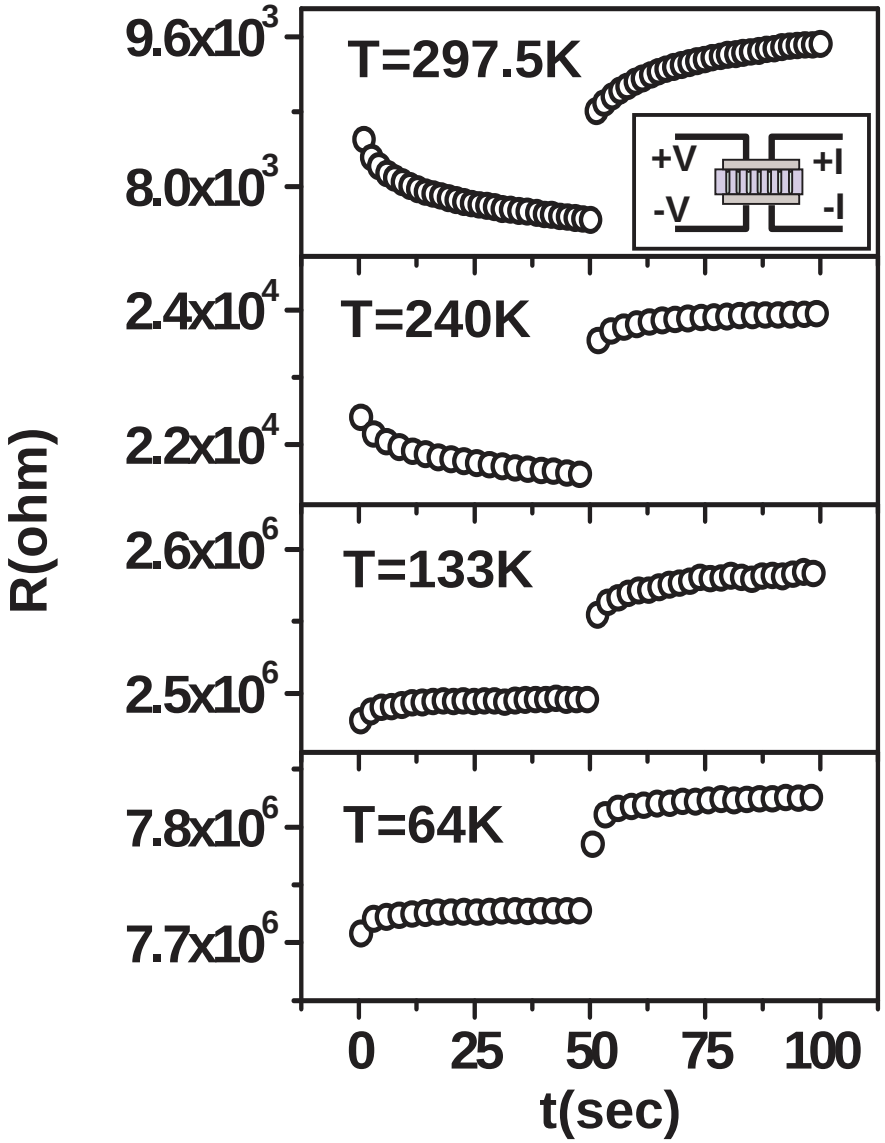
9.6x10^3
8.0x10^3
T=297.5K
+V
+I
-V
-I
2.4x10^4
2.2x10^4
T=240K
2.6x10^6
2.5x10^6
T=133K
7.8x10^6
7.7x10^6
T=64K
R(ohm)
0
25
50
75
100
t(sec)

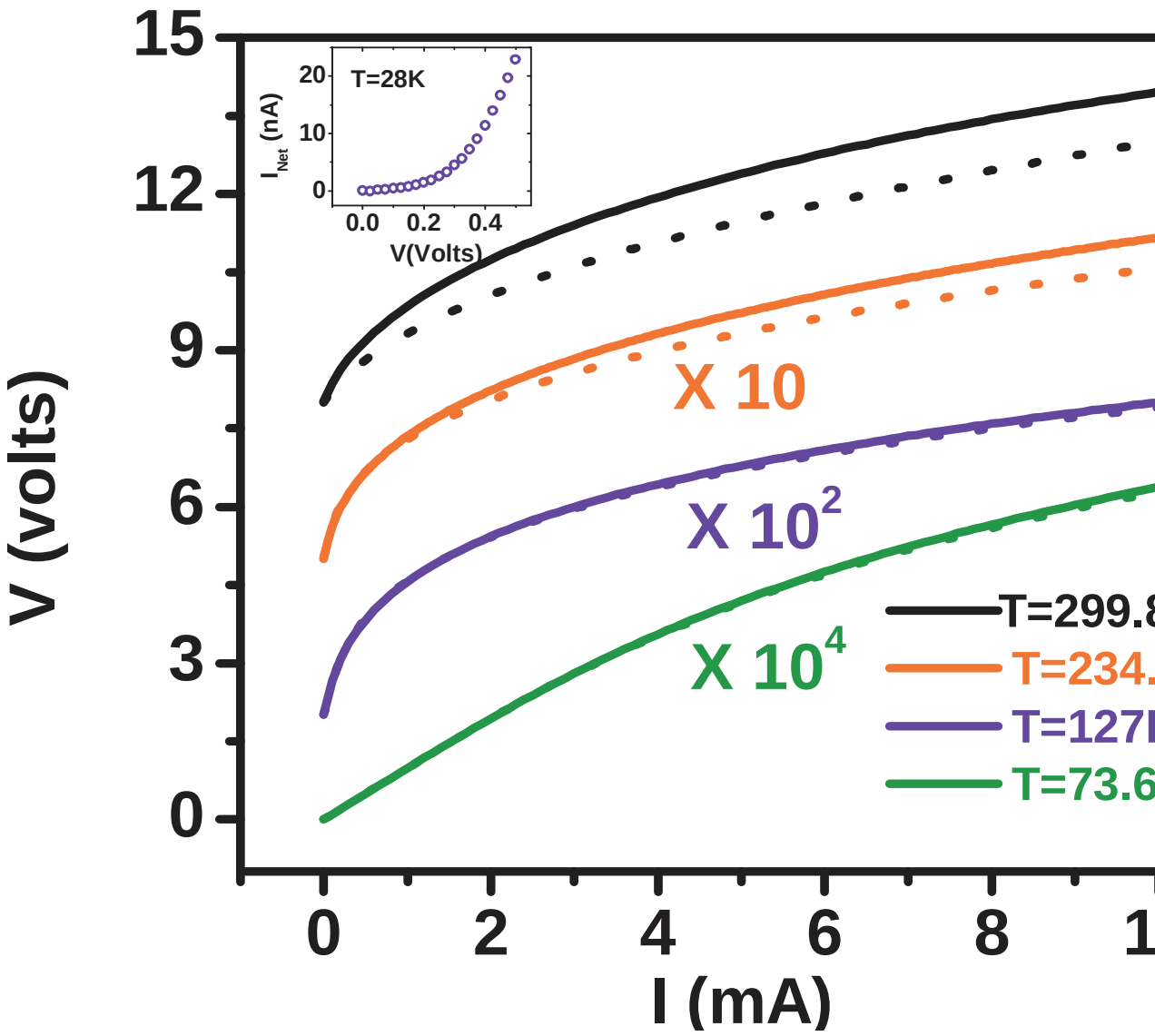
15
12
9
6
3
0
V (volts)
0
2
4
6
8
1
I (mA)
T=28K
20
10
0
0.0
0.2
0.4
V(Volts)
I_Net (nA)
X 10
X 10^2
X 10^4
T=299.8
T=234.
T=127
T=73.6

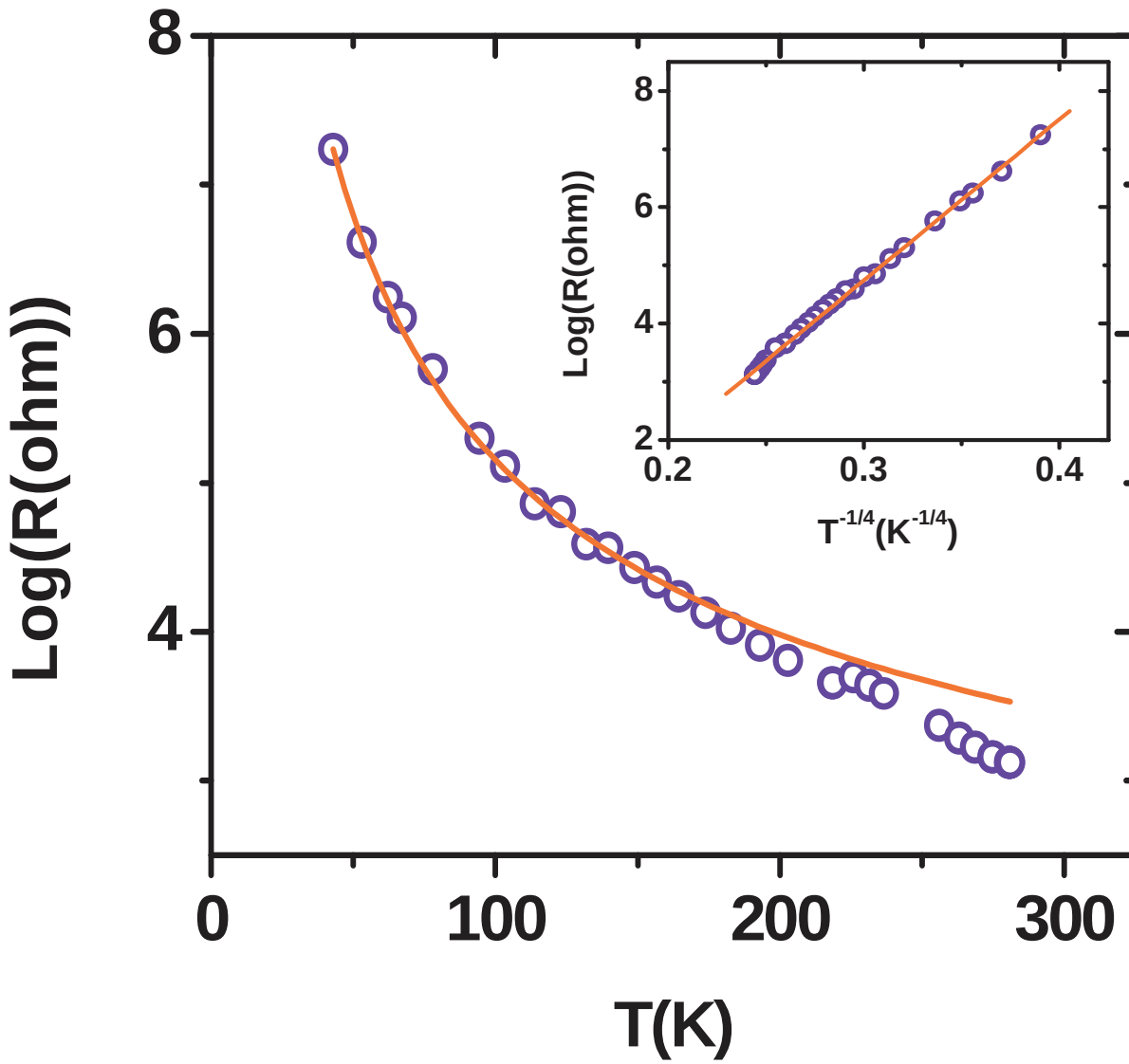
Log(R(ohm))
T(K)
8
6
4
0
100
200
300
Log(R(ohm))
T^-1/4(K^-1/4)
8
6
4
2
0.2
0.3
0.4

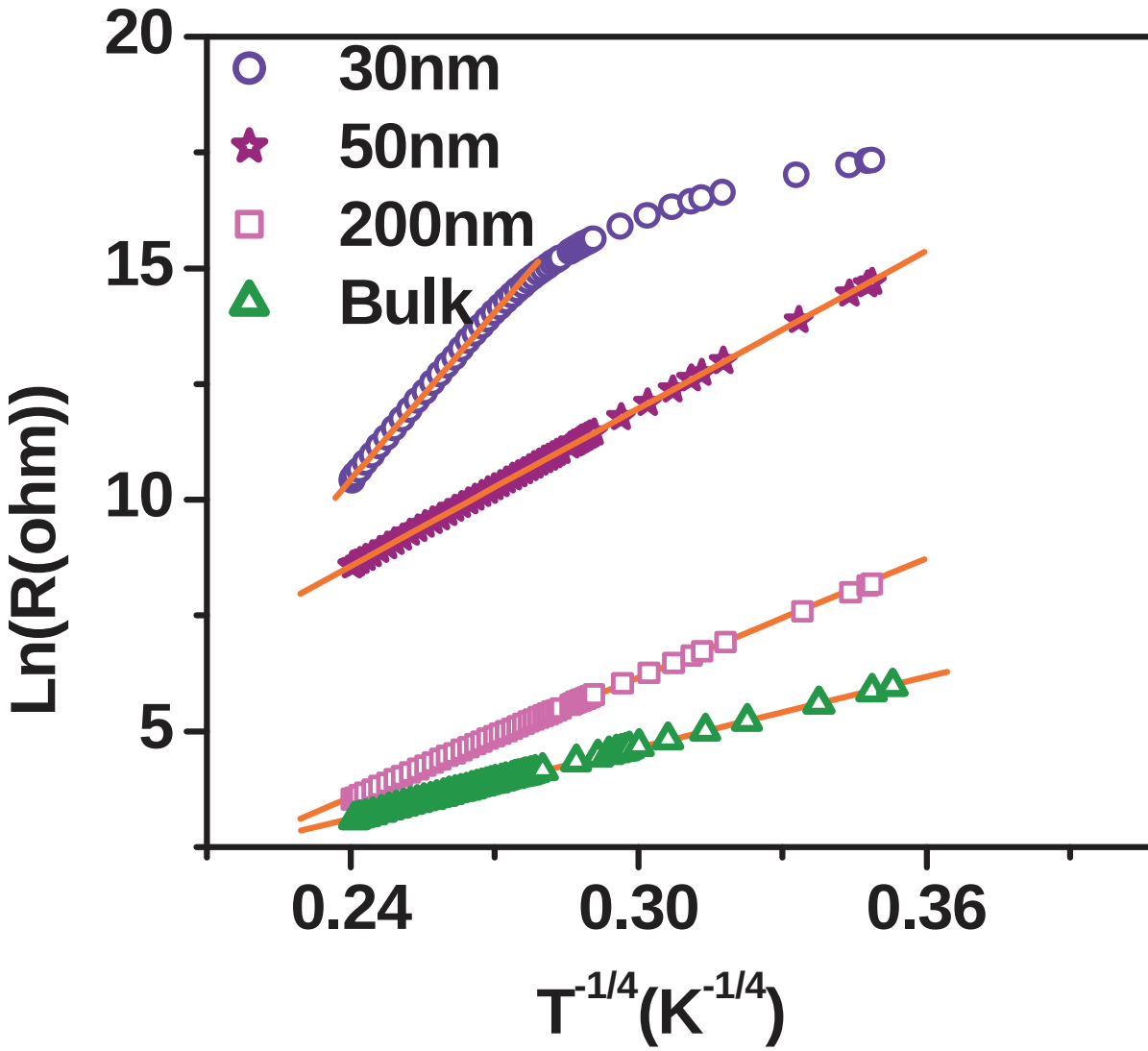
20
15
10
5
Ln(R(ohm))
30nm
50nm
200nm
Bulk
0.24
0.30
0.36
T-1/4(K-1/4)

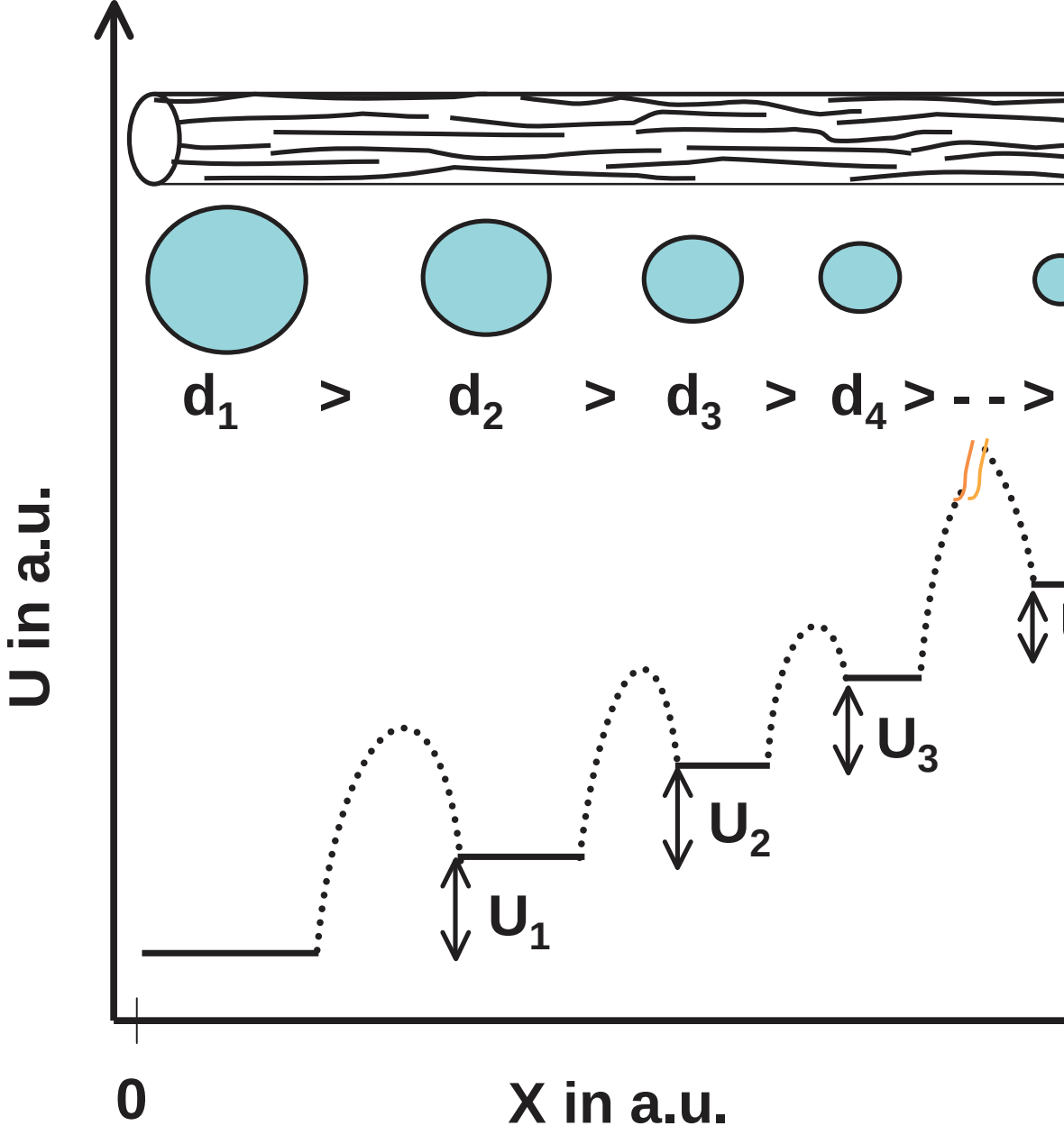
d1 > d2 > d3 > d4 > - - >
U in a.u.
U1
U2
U3
0
X in a.u.

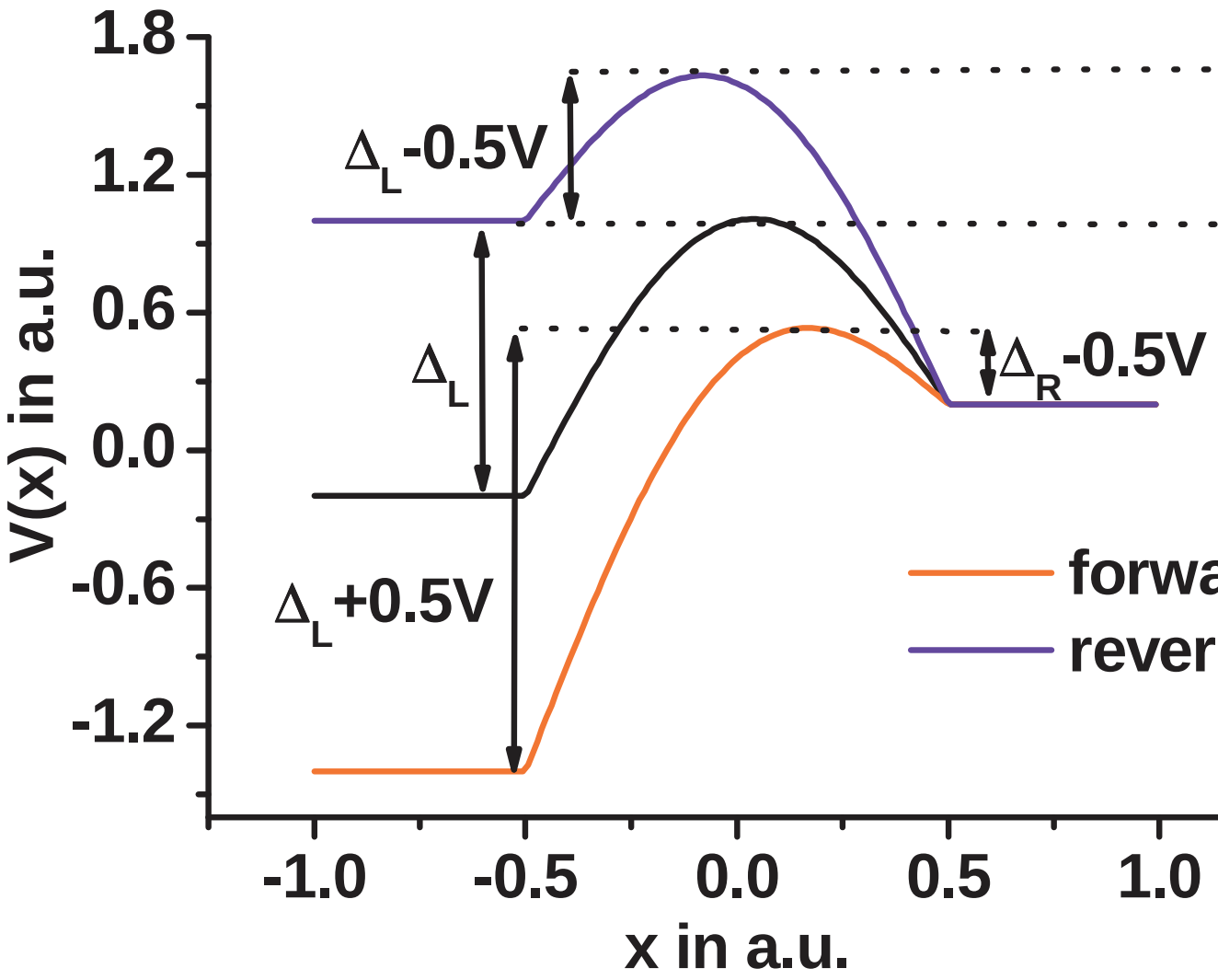
1.8
1.2
0.6
0.0
-0.6
-1.2
V(x) in a.u.
-1.0
-0.5
0.0
0.5
1.0
x in a.u.
Δ_L -0.5V
Δ_L
Δ_L +0.5V
Δ_R -0.5V
forwa
rever

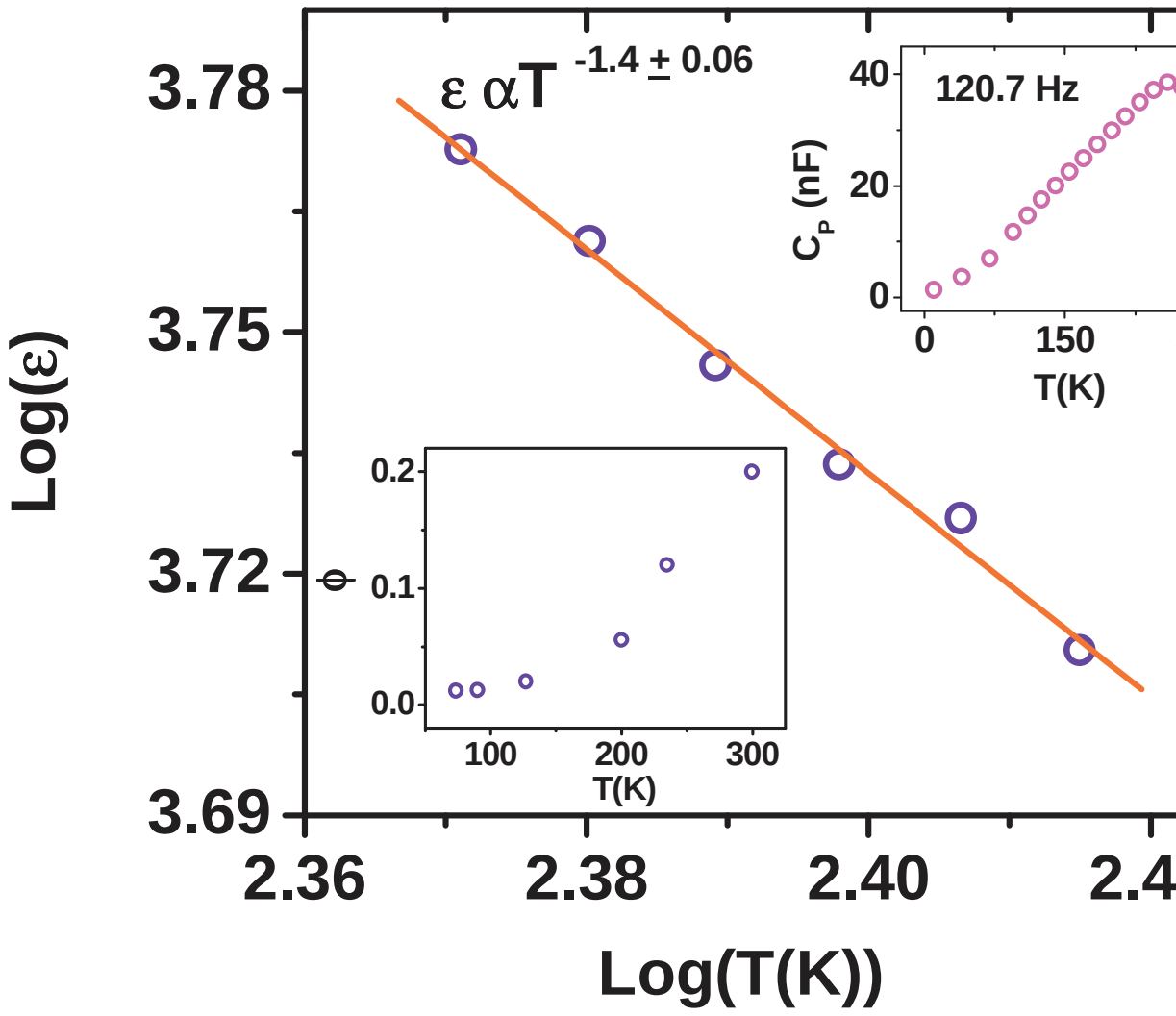
ε αT -1.4 ± 0.06
3.78
3.75
3.72
3.69
Log(ε)
2.36
2.38
2.40
2.4
Log(T(K))
120.7 Hz
40
20
0
C_P (nF)
0
150
T(K)
0.2
0.1
0.0
ϕ
100
200
300
T(K)